# Use of a Scanning Probe Microscope to Measure Marring Mechanisms and Microhardness of Crosslinked Coatings

Weidian Shen, Stanley M. Smith, Frank N. Jones, and Caigui Ji—Eastern Michigan University*
Rose A. Ryntz and Mark P. Everson—Ford Motor Company†

*A scanning probe microscope (SPM) was equipped with a high-modulus probe to indent coating surfaces when normal force is applied. A method for measuring microhardness with this probe is described. The high-modulus probe was also used to mar coating surfaces under controlled conditions by application of normal force plus lateral motion. Dimensions of the mars were measured by conventional scanning probe microscopy. The data were analyzed in terms of a "three response, two mechanism model" of marring in which three types of responses of polymeric materials: elastic, plastic deformation, and fracture, are measured. Of the three responses, only plastic deformation and fracture result in marring, and the two mechanisms can be quantified. A fourth quantity which combines plastic deformation and fracture is suggested as a method of comparing "micro mar resistance" of materials under specified conditions. Three crosslinked polymeric coatings were studied in detail. Two had hard crusts of material near their surfaces that responded quite differently than the bulk of the material.*

## INTRODUCTION

We previously described[1,2] a modified scanning probe microscope (SPM) that can be used to mar polymer surfaces under controlled conditions and the use of conventional scanning probe microscopy to measure the dimensions of the mar. Here we report on the use of an SPM to quantitatively characterize the responses of coating surfaces to marring stress. A method of measuring microhardness using the SPM as a microindenter is also discussed.

Terminology recommended by Courter[3] is used in this study; ASTM[4] terminology is similar. The terms "mar" and "marring" are used to describe surface defects that are large enough to degrade the appearance of a polymer surface but are small with respect to the coating thickness. For example, mars 0.2 to 0.5 μm deep and 1 to 2 μm wide degrade the appearance of automobile clearcoats that are 30-60 μm thick.[1,2] Mar resistance is a measure of a material's ability to resist appearance degradation caused by small-scale mechanical stresses under a specific set of conditions. Other authors use the terms scratch resistance, abrasion resistance, wear resistance, and erosion resistance to mean more or less the same thing. Of the possible terms, mar resistance seems the least ambiguous and is, therefore, preferred.

In this study we adopted a "three response, two mechanism" model for marring. It is derived from studies of the physics of microhardness and of marring of polymers described by Briscoe et al.[5-8], by Balta Callega et al.[9-11], and by other authors.[12-15] In our model a surface may undergo three types of response under physical stress: elastic, plastic deformation (or "plastic flow"), and fracture. Briscoe et al. used the terms "elastic response," "elastic-viscoplastic response (yield)," and "fracture deformations" to describe "the three main responses during scratch deformation."[8] While their terminology is different, the meaning appears similar. Of these three responses, only two, plastic deformation and fracture, cause marring. No marring results from the elastic response because the surface recovers its original dimensions almost instantaneously when the stress is removed.

The three response, two mechanism model is simplistic. Complete analysis of the response of polymeric materials to mechanical stress involves a multitude of variables.[14] Among the complexities not accounted for in our model are the viscoelastic creep,[11] which may cause slow (partial) recovery of the original dimensions after

*430 W. Forest Ave., Ypsilanti, MI 48197.
†401 Southfield Rd., Dearborn, MI 48121-6231.

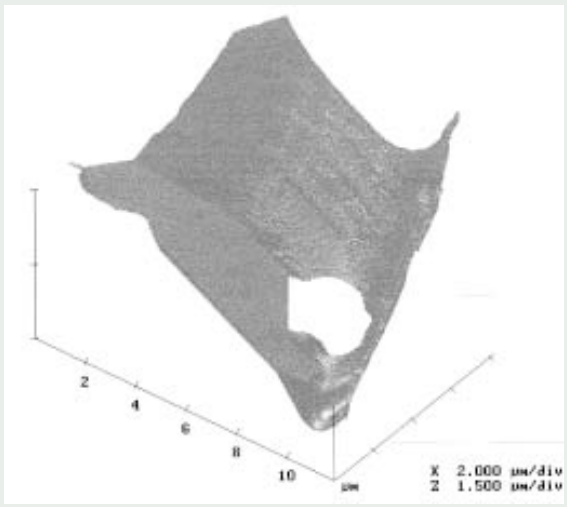


*Figure 1—3-D picture of the diamond tip used in the test.*

plastic deformation. Also, some authors differentiate two types of fracture: tearing and cracking.[7] Briscoe[5] proposed a more elaborate model for friction and wear. Physical models characterizing the width[9,10,16] and depth[8,13,16] of mars resulting from plastic deformation have been proposed. Such models accommodate the likely situation in which the material undergoes a mixture of plastic and elastic responses. Physical models for brittle[14] and ductile[15] fracture have been described. By disregarding these additional complexities, it becomes possible to differentiate two main mechanisms of marring and to measure them quantitatively.

Mar resistance is an important property of the coatings used on automobile bodies, appliances, eyeglass lenses, polycarbonate glazing, and vinyl flooring. Often it proves difficult to relate the mar resistance of a given material to readily measurable basic properties. Investigators frequently resort to empirical laboratory tests which, it is hoped (often very optimistically), will correlate with service experience. For example, one empirical test[17,18] employs an "AATCC Crockmeter" to rub a surface with a felt pad filled with a dry abrasive household cleaning compound; the mar resistance is taken as the percent reduction in the 20° gloss of the rubbed area. This test is recognized to have limitations, but it continues in wide use because it is simple to perform and it correlates to some extent with the ability of a coating to withstand marring in a car wash. Morse[19] described many other empirical mar resistance tests that have been adopted as standards for various types of coatings. Generally, these empirical tests share significant limitations—the marring stresses are poorly characterized and the data analysis does not discriminate between the common marring mechanisms, plastic deformation, and fracture.

As reviewed in 1996 by Courter,[3] some coatings researchers have tried to relate mar resistance to basic polymer properties. For example, Gregorovich and McGonigal[20] and Betz and Bartelt[21] correlated tensile properties and polymer structures with mar resistance. These authors recognized two distinct mechanisms of marring: plastic deformation and brittle fracture (called "non-abrasive" and "abrasive" scratches, respectively, by Betz and Bartelt). They distinguished these mechanisms qualitatively by scanning electron microscopy. Betz and Bartelt emphasized an additional complication: mars may partly or even completely heal ("reflow") with time, especially if the coating is heated. Presumably healing results from viscoelastic creep of materials that have undergone partly elastic and partly plastic deformation. Various authors have correlated mar resistance with crosslink density,[22-24] network homogeneity,[21] $T_g$,[22,23,25] modulus,[26,27] toughness,[3,26,27] hardness,[23,24,27] coefficient of friction,[27] and the presence of additives that harden the surface,[23,24] lubricate it,[5,27,30] or promote healing.[21] While some of the studies provide useful insights, they are limited by the

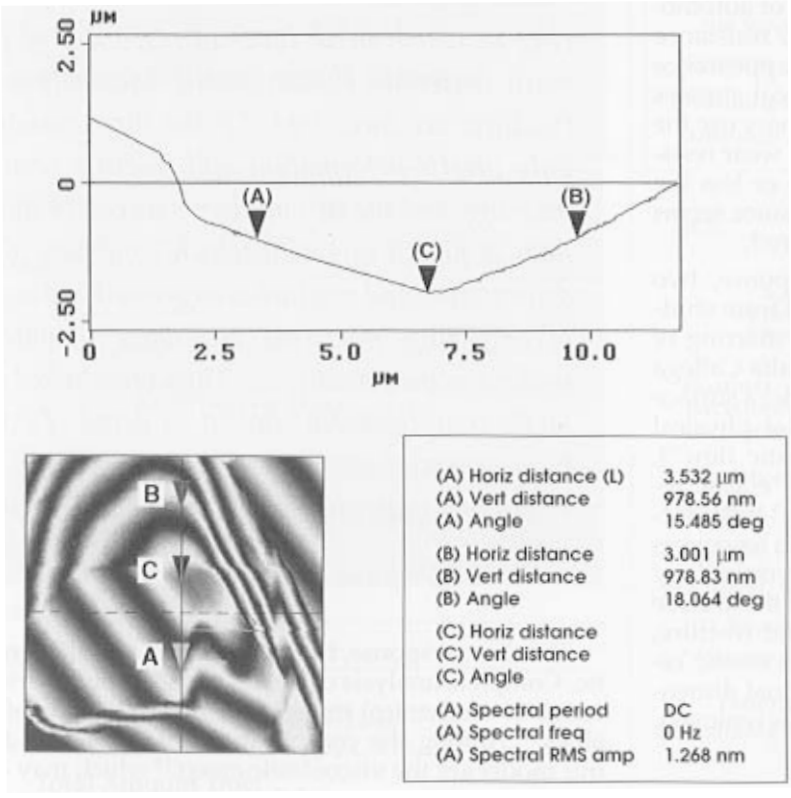


*Figure 2—The cross-section profile of the tip along the direction perpendicular to the direction of the marring in the test.*

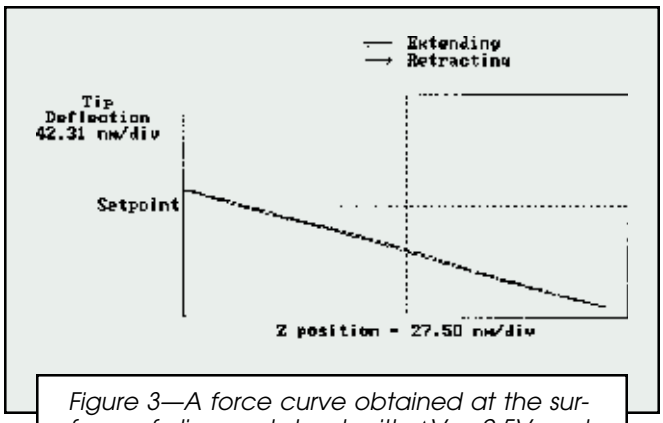


*Figure 3—A force curve obtained at the surface of diamond sheet with ΔV = 2.5V and corresponding $\Delta Z_{dmnd}$ = 455nm.*

fact that they usually correlate one or several basic polymer properties with empirical mar resistance tests that have the limitations described previously. It is no wonder that the overall picture that emerges is unclear and sometimes seems to lead to contradictory conclusions.

Many researchers have sought better methods for characterizing marring. For example, Kody and Martin[31] used advanced light scattering techniques coupled with digital image analysis to characterize mars in polypropylene composites. The mars were made under controlled conditions with a stylus, and the analysis provides information about the mechanisms of deformation.

Here we describe a new mar resistance test in which the marring stress is applied with controlled force and rate and in which the data analysis provides a quantitative measure of the fraction of elastic response, plastic deformation, and fracture under the conditions of the test. The test employs a modified scanning probe microscope (SPM) to mar the material and conventional scanning probe microscopy to measure and characterize the results. The modification consists of installing on the SPM a specially fabricated probe consisting of a diamond tip mounted on a high-modulus tungsten cantilever; this probe is stiff enough to indent most polymer surfaces under the normal forces that can be applied with an SPM and to mar surfaces when normal force is combined with lateral movement. Thus, it can be used both as a microhardness tester and as a device for marring polymer surfaces with known force and velocity.

## EXPERIMENTAL DETAILS

### Specimens Tested

The study focused on three specimens prepared in our laboratory by casting films of unpigmented coatings on aluminum panels using a #26 wire-wound bar and crosslinking them for 30 min at the recommended temperatures, 120 to 150°C. The coatings' thickness measured 15-20 μm. These specimens were selected to exemplify a variety of responses. *Coating PE* comprised a polyester resin, made in our laboratories, crosslinked with a monomeric methylolated melamine formaldehyde resin under acid catalysis; this coating is highly elastic. *Coating PU* was an experimental coating, described as a polyurethane, obtained from DuPont in two components, coded RKR94550 and RK7018 which were mixed in our laboratory just before films were cast. Under various marring stresses it may undergo elastic, plastic, and fracture responses. *Coating AC* was a commercial, one-component automotive clearcoat obtained from DuPont and coded "Gen-3." It is presumed to be based on special acrylic polymers crosslinked, at least partly, with alcoholated melamine-formaldehyde resins. It exemplifies a relatively mar resistant commercial automotive clearcoat.

Other coatings, some made in our laboratories and others provided by PPG Industries, Inc. were also examined to illustrate marring that occurs in the field.

### Preparation of High-Modulus Probe

A cantilever was cut from a piece of tungsten foil of 12.7 μm thickness. It was rectangular with dimensions of 572 × 435 μm. To make the tip, a thin piece of diamond was shattered and a roughly pyramidal shard was selected. It was affixed to the cantilever with epoxy cement. The assembled probe was inverted and imaged with a conventional SPM tip; *Figure* 1 shows a projection of a three-dimensional image of the diamond tip of the probe, and *Figure* 2 shows the cross-section profile of the tip along the direction perpendicular to the direction of travel in the mar test.

### Force Calibration

The high-modulus probe was mounted on a Digital Instruments "Nanoscope III" SPM. A thin, flat piece of diamond was mounted on the sample holder. The diamond sheet was pushed upward against the diamond tip with 10 different levels of normal force. In the force calibration mode of the SPM, instrument readout is in terms of voltage, V, and a change in voltage is proportional to the force exerted on the probe. Suppose $V_o$ is the signal before the diamond sheet touches the tip of the probe and $V_{stpt}$ is the signal after the sheet touches the tip and deflects the cantilever to a certain extent. The

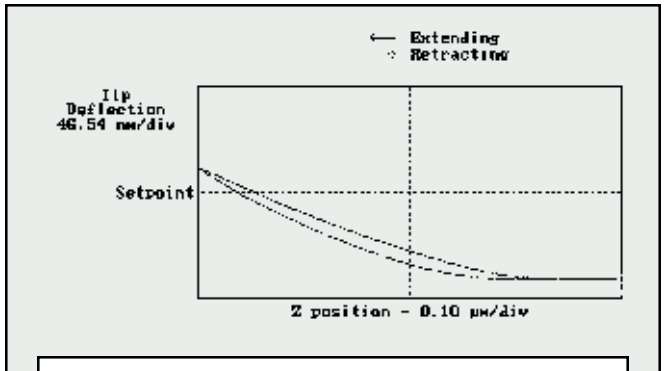


*Figure 4—A force curve obtained at the surface of coating PE with ΔV = 2.5V and corresponding $\Delta Z_{ctg}$ = 1433nm.*

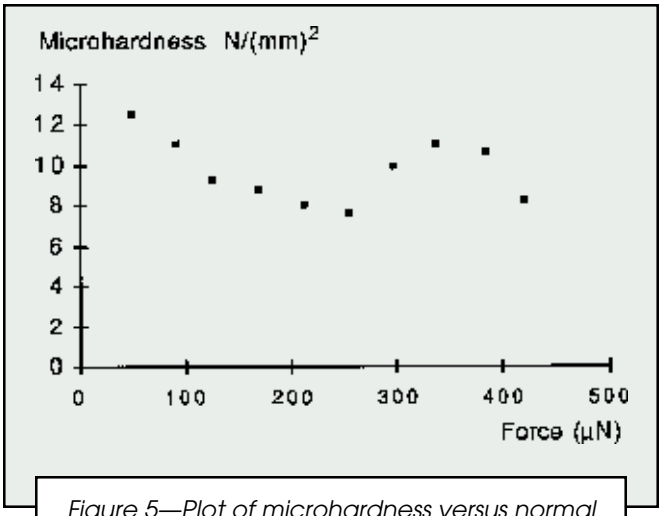


*Figure 5—Plot of microhardness versus normal force for coating PE.*

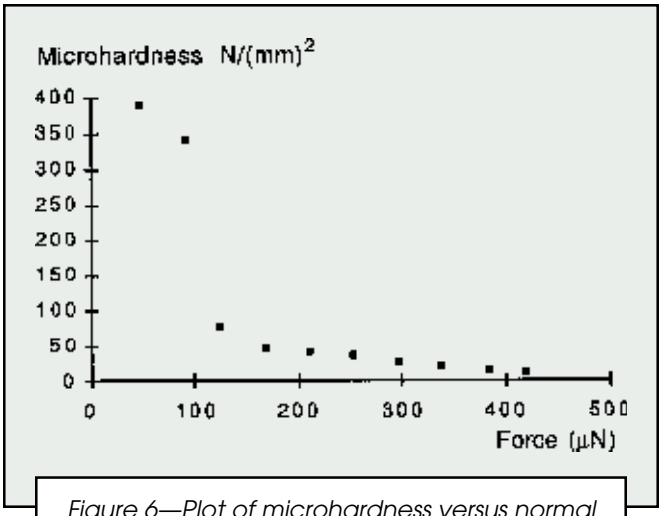


*Figure 6—Plot of microhardness versus normal force for coating PU.*

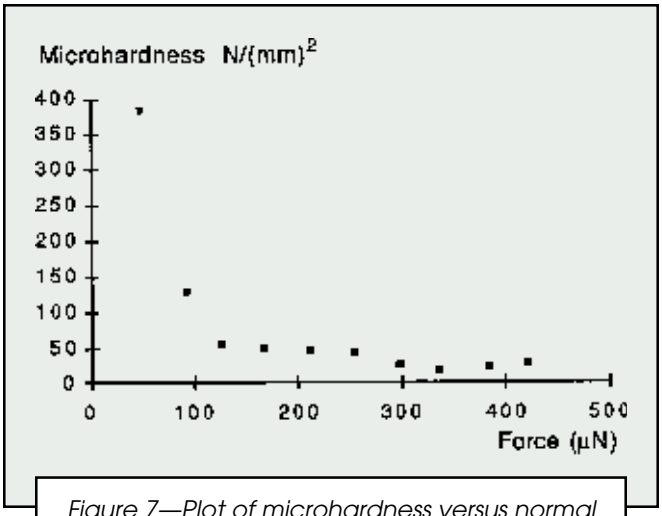


*Figure 7—Plot of microhardness versus normal force for coating AC.*

feedback loop of the instrument was set to maintain a specific deflection during subsequent marring experiments. $V = V_{stpt} - V_o$ reflects the normal force applied to the tip. Forces varying from V = 0.5 V to V = 5.0 V were exerted in 10 steps and the vertical advancements of the diamond sheet were recorded and used to construct a force curve in which the deflection of the cantilever is plotted versus the vertical advancement of the diamond sheet. As illustrated in *Figure* 3, an advancement of 455 nm ($Z_{dmnd}$ = 455 nm) by the sheet against the tip yields a signal of V = 2.5 V.

The diamond tip and sheet are assumed to be non-deformable under these conditions; therefore, all vertical sample motion is transferred to cantilever deflection. The normal force in this instance is given by FN = K * $Z_{dmnd}$ = 465 N/m * m 455 = 212 μN. The spring constant, K, of the assembled tip used in this study was calculated to be 465 N/m using equation (1):

$$K = E\frac{Wt^3}{4L^3} \quad (1)$$

E is Young's modulus and L, W, and t are the length, width, and thickness of the cantilever. For comparison, the spring constants of the SPM cantilevers used for conventional SPM surface imaging are in the range 0.06 to 0.6 N/m.

### Measurement of Depth of Indentation and Calculation of Microhardness, $H_{mic}$

Coating samples were placed on the sample holder of the SPM and were advanced against the stiff probe at the same 10 levels of normal force. *Figure* 4 shows the force curve for *coating PE* with V = 2.5V. In this case a vertical advancement of the coating of 1,433 nm ($Z_{ctg}$ = 1,433 nm) was needed to produce the same cantilever deflection as was produced by a vertical advancement of 455 nm ($Z_{dmnd}$ = 455 nm) by the diamond sheet under these conditions. The difference, in this case 978 nm, is attributed to penetration of the coating by the diamond tip of the probe. The depth of penetration of each coating was measured under normal forces of 49, 92, 126, 169, 212, 254, 298, 338, 385, and 421 μN.

To calculate microhardness the depth of penetration and the profile of the diamond tip, measured earlier, are used to calculate the area of the coating surface in contact with the tip after deformation as it presses a given distance into a polymeric material. Note that the area in contact with the tip was used in this calculation, not the planar area of the surface affected by the tip before the surface was disturbed. In these calculations the tip is assumed to be conical with the cross-section dimensions shown in *Figure* 2. The procedure is described by example. In *Figure* 2 the vertical depth between the left cursor and the middle cursor and between the right cursor and the middle cursor are 979 nm. These distances are about the same as the depth of indentation of *coating PE* at $F_n$ = 212 μN. Therefore, the triangle formed by the three cursors is the cross-section of the part of the tip stuck into *coating PE* at $F_n$ = 212 μN. Microhardness is given by $H_{mic} = F_n/A_{cont}$ where $A_{cont}$ is the contact area between the coating and the tip. Assuming that the tip is

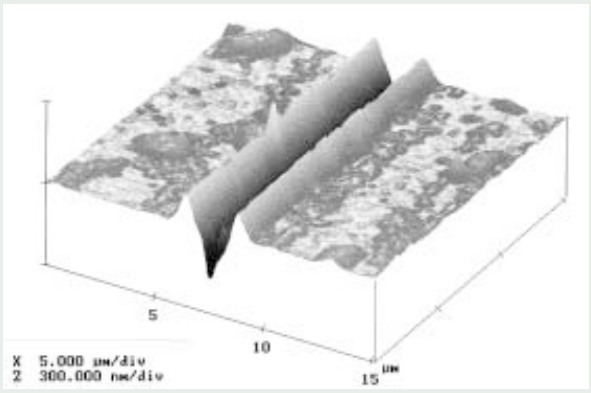


*Figure 8—A typical mar at the surface of a coating in which plastic deformation dominates.*

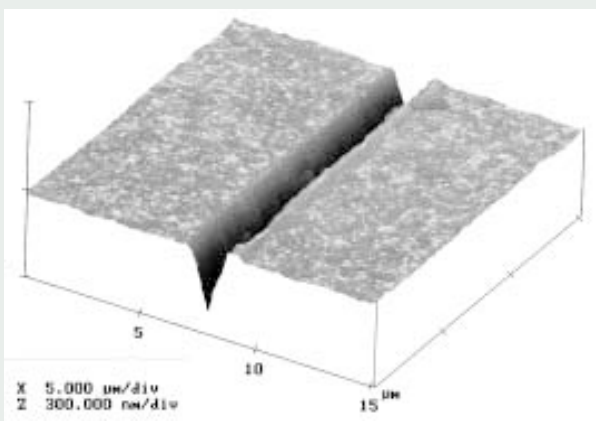


*Figure 9—A typical mar at the surface of a coating in which fracture dominates.*

cone-shaped, $A_{cont} = \pi_{avg} l_{avg}$. The radius of the cone, r, is the horizontal distance between the left or right cursor and the middle cursor in *Figure* 2, and the length of the side of the cone, l, is the distance between the left or right cursor and the middle cursor in *Figure* 2. By measuring and averaging r and l at the same depth along different directions $r_{avg}$ and $l_{avg}$ were obtained. From these quantities $A_{cont}$ can be calculated and used to calculate $H_{mic}$. Data for *coatings PE, PU*, and *AC* are given in *Table* 1 and are plotted in *Figures* 5-7.

### Hardness Measurements by Conventional Dynamic Loading Technique

For comparison, *coatings AC* and *PE* were studied using a Fischerscope H100 Micro-Hardness Tester equipped with a Vickers indenter using the dynamic loading technique described by Weiler.[32] Note that the dimensions of the Vickers indenter are much larger than those of the diamond tip, and comparisons may not be valid.

### Methods of Marring Surface: Qualitative Characterization of Marring Mechanism

A coating specimen was mounted on the sample holder of the SPM and advanced against the high-modulus probe to a normal force of 49 µN. The feedback loop was set to maintain the normal force. The sample was then moved back and forth at a frequency of 0.5 Hz to make five bi-directional scrapes 70 µm long in the same track. The result is one mar. In preliminary experiments it was determined that more reproducible results were obtained by using 10 scrapes than by using a single scrape. Velocity of the motion was 0.07 mm/sec. The probe was then moved by about 8 µm, normal force was increased to 92 µN, and the procedure was repeated to make a second mar parallel to the first. This process was continued until 10 mars were made in the specimen with applied normal forces of 49, 92, 126, 169, 212, 254, 298, 338, 385, and 421 µN. The specimen was removed and cleaned in an unheated ultrasonic bath containing water and detergent, rinsed in a stream of cool tap water, gently dried with soft tissue, and blown dry with high pressure nitrogen. This cleaning procedure removed all loose debris. It was determined that the dimensions of mars in these three coatings are unaffected by this cleaning procedure; however, mars in certain other coatings become smaller if they are immersed in water, and in such cases this cleaning procedure should not be used.

The high-modulus probe was replaced with a conventional SPM probe and the instrument was used in the conventional contact mode[33] to image the mars. The elapsed time between marring and imaging was about one hour. Images of mars produced in typical coatings are shown in *Figures* 8-9, and a typical cross-section is shown in *Figure* 10. Results for *coatings PE, PU*, and *AC* are shown in *Figures* 11-13. Note that the vertical scale in these figures is magnified relative to the horizontal scale. The procedure was repeated three or more times on each of the three coatings, and the results were reproducible.

A second method of marring the surface was to set the SPM to raster forward by 0.137 µm after each lateral marring motion. The result was a 70 × 70 µm square in the surface of the material which had been subjected to 512 closely adjacent marring stresses. The same cleaning procedure was used. Typical results are shown in *Figures* 14 and 15.

### Quantitative Characterization of Responses to Marring Stress

The dimensions of each mar made by the first procedure described previously were measured in 10 places using the zoom-in function of the SPM. It was found that the cross-sections of the ditches and of the shoulders (if any) of the mars could be closely approximated as triangles. The areas of the cross-sections of each ditch ($A_{dit}$) and of the sum of the two shoulders ($A_{shs}$) were calculated at the 10 places in each mar. The results, which were closely distributed, were averaged for each mar. Note that $A_{dit}$ excludes the area between the shoulders, if any. A third cross-section area, $A_{ind}$, was calculated from the depth of the indentation measured during microhardness measurements and the dimensions of the diamond tip of the high-modulus probe. A fourth cross-

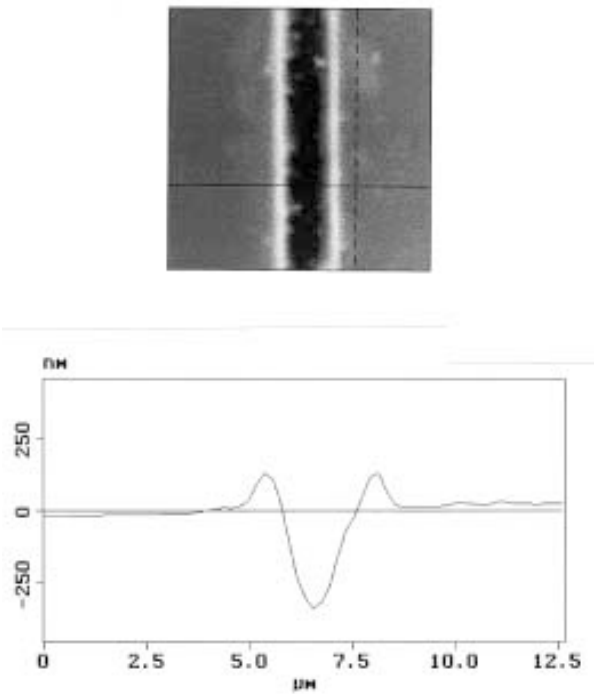


*Figure 10—An image of a mar and its cross-section profile of a coating which fails by both plastic deformation and fracture.*

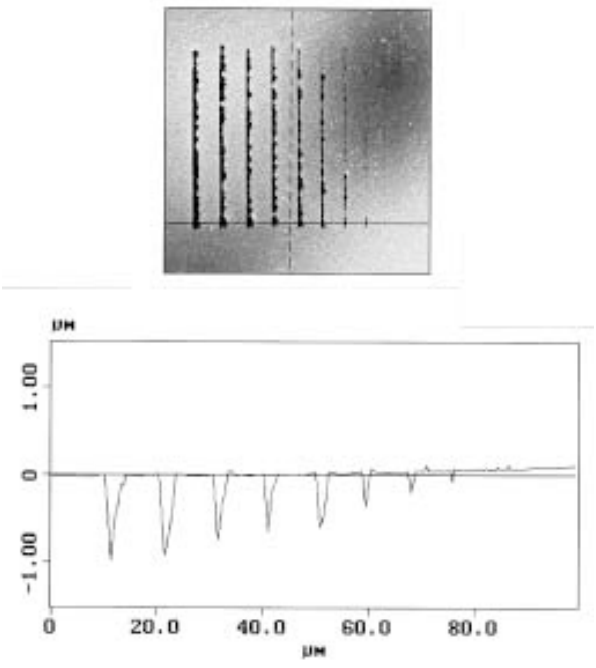


*Figure 11—Image of the mars made under normal forces of 49μN, 92μN, 126μN, 169μN, 212μN, 254μN, 298μN, 338μN, 385μN, and 421μN, and their cross-section profile at the surface of coating PE.*

section area, $A_{tro}$, was calculated as the area of the mar including the area between the shoulders. These areas are illustrated schematically in *Figure* 16. The use of these areas to quantify the responses is described in the Results Section of this paper.

### Empirical Mar Resistance Test

A procedure adapted from published procedures[17,18] was used. Test panels were prepared by coating 4 × 6 in. aluminum panels with a glossy commercial black paint, Rust-Scat™ from Coronado Paint Co. The black paint films were cast on the panels using a #26 wire-wound bar followed by baking for 30 min. at 143°C. Coating films were then cast on the black test panels by the same method; coatings baked at the same temperatures used to prepare specimens for SPM testing. The coated panel was heavily dusted with dry Bon-Ami™ cleaning powder and the excess powder was gently poured off. The panel was mounted on an "AATCC Crockmeter, Model CM-1" supplied by Atlas Co. The dowel shaped, Plexiglass probe with a flat, 15 mm-diameter tip supplied with the device was used. The Crockmeter was modified by gluing a magnetic strip in front of the test bed to mechanically hold the panel in place. A fresh green 50 × 50 $mm^2$ felt pad, also supplied by Atlas, was fastened to the probe of the Crockmeter with a spring clip. The test probe was stroked back and forth over a portion of the panel in 10 double strokes at a frequency of about one double stroke per second, leaving a marred area of about 13 × 220 mm. The panel was cleaned in a stream of cool tap water, gently wiped with a wet wiper, and gently dried with a soft towel. The 20° gloss was measured using a micro-TRI-gloss™ pocket gloss meter (supplied by BYK-Gardner, Inc.) by slowly moving the meter across the panel, measuring the gloss of the marred center and the unmarred sides of the panel. Measurement was repeated three times on different parts of each panel. Results were estimated to be reproducible to within ± 5%. The results were averaged and recorded as percent gloss retained by the marred area.

## RESULTS

### Preparation and Calibration of High-Modulus Probe, Measurement of Depth of Indentation, and Calculation of Microhardness, $H_{mic}$

Preparation and calibration of the high-modulus tip and measurement of $H_{mic}$ were described earlier. The $H_{mic}$ results for the three coatings are given in *Table* 1 and are displayed in *Figures* 5-7. The success of the method depends upon its ability to measure the deflection of the cantilever caused by each applied normal force and to separate deformation caused by penetration of the tip into the polymer specimen during hardness measurement from the advancement of the sample against the tip. The technique yields microhardness measurements in basic physical units, $N/mm^2$, but several assumptions (non-deformability of the diamond tip and diamond sheet, conical cross-section of the tip, and no change in geometry caused by bending of the cantilever as force is

**Table 1—Microhardness in the Units N/(mm)$^2$ of Coatings PE, PU, and AC Under 10 Different Normal Forces in Units μN**

| Force (μN) | Microhardness Coating PE (N/mm*mm) | Coating PU (N/mm*mm) | Coating AC (N/mm*mm) |
|---|---|---|---|
| 49 | 12.5 | 390 | 385 |
| 92 | 11 | 338 | 129 |
| 126 | 9.24 | 75.6 | 53 |
| 169 | 8.75 | 45 | 49.7 |
| 212 | 8 | 41.4 | 46.8 |
| 254 | 7.6 | 35 | 43.9 |
| 298 | 9.89 | 25.6 | 25.1 |
| 338 | 11 | 20.8 | 16.7 |
| 385 | 10.6 | 15.8 | 23.1 |
| 421 | 8.2 | 11.4 | 28.8 |

increased) modestly reduce the absolute precision of the measurements. The method, in its present state of development, is judged capable of giving approximate absolute microhardness measurements and relative measurements that are very reliable for comparisons of different polymer specimens. With refinement, the absolute precision of the method could be improved.

Microhardness of *coatings PU* and *AC* by the SPM method are similar (compare *Figures* 6 and 7). In these cases the microhardness is 385 - 390 N/mm$^2$ at the lowest force (49 μN), drops precipitously at forces of 92 - 126 μN, levels out at about an order of magnitude lower than the initial reading at forces of 169 to 240 μN and decreases by another 50% at higher forces. Apparently, these coatings have a thin crust that is much harder than the bulk of the material. C*oating PE* behaves quite differently (see *Figure* 5); its microhardness is lower than that of the other two coatings by a factor of 30 at a force of 49 μN. However, its microhardness drops only about 50% as force is increased to 212 μN and then increases slightly at higher force. At forces of 298 - 421 μN, $H_{micind}$ of *coating AC* is about 1.5 to 2.5 times harder than *coating PE*.

For comparison, micro indentation hardness of *coatings PE, PU*, and *AC* were measured by a conventional dynamic loading method[32] using a commercial instrument equipped with a Vickers indenter. The results are summarized in *Table* 2. There are qualitative similarities between the results of the two methods. With *coatings PE, PU*, and *AC*, microhardness measured by SPM drops sharply as the probe penetrates more deeply into the specimen. The dynamic loading method confirmed the *coating AC* is two to four times harder than coating PE at normal forces in the range 300 to 400 μN.

### Methods of Marring Surfaces: Qualitative Characterization of Marring Mechanisms

Each mar was made by scraping a path 10 times with the high-modulus probe. In preliminary experiments 10 scrapes proved to give more reproducible results than a single scrape. (In later studies we found that five scrapes are sufficient.) Qualitative indications of the mechanisms of marring can be obtained by inspection of mars observed on typical coatings (*Figures* 8-10) and of the par-

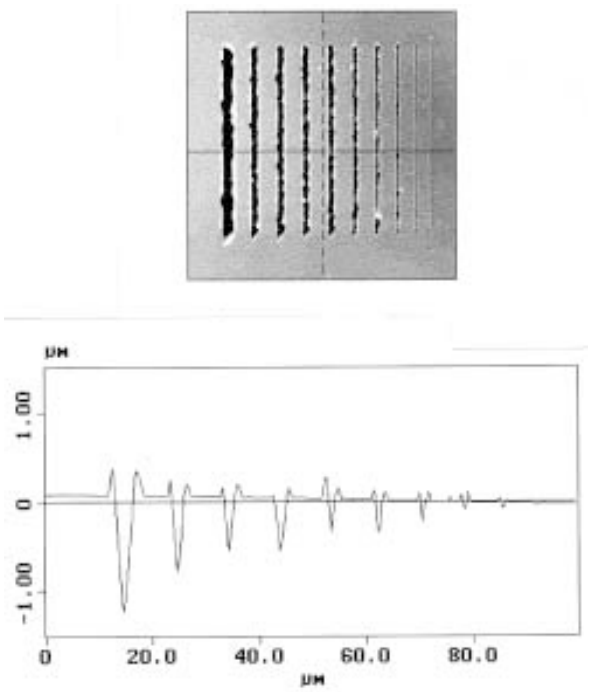


*Figure 12—Image of the mars made under normal forces of 49μN, 92μN, 126μN, 169μN, 212μN, 254μN, 298μN, 338μN, 385μN, and 421μN, and their cross-section profile at the surface of coating PU.*

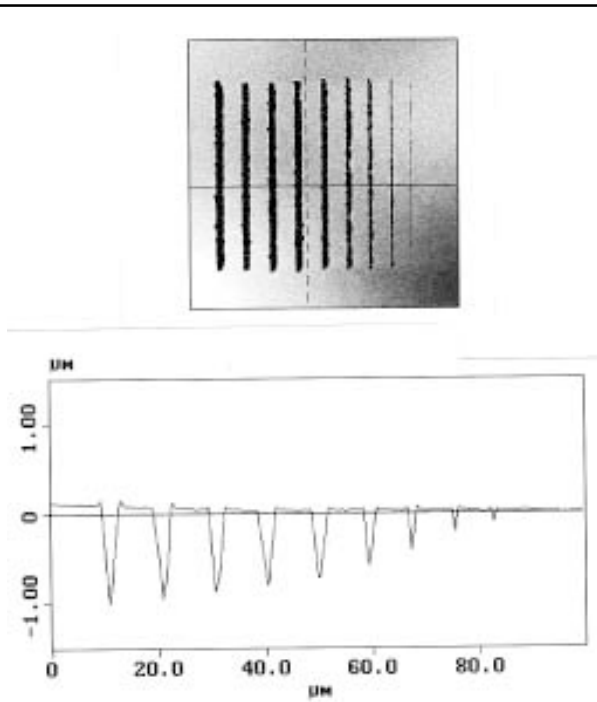


*Figure 13—Image of the mars made under normal forces of 49μN, 92μN, 126μN, 169μN, 212μN, 254μN, 298μN, 338μN, 385μN, and 421μN, and their cross-section profile at the surface of coating AC.*

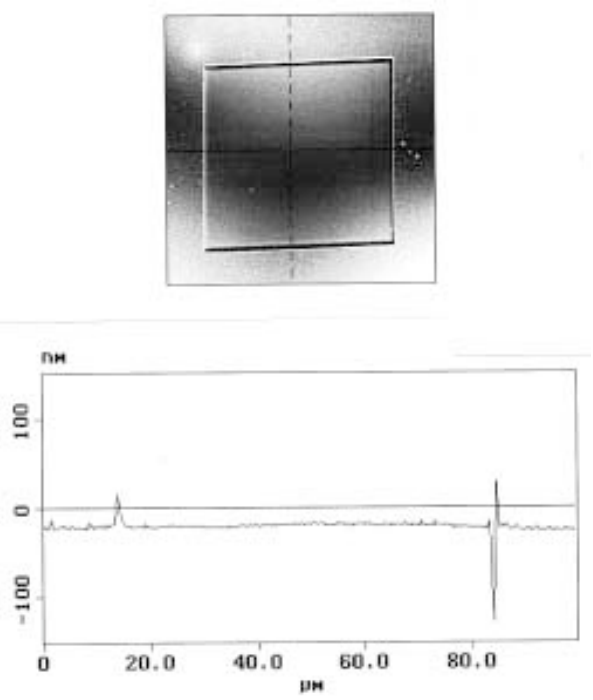


*Figure 14—(a) A plastic deformation dominate area of 70μ x 70μ, in which 512 vertical mars have been made from the left side to the right side; (b) its cross-section profile, in which only the left shoulder of the first mar and the ditch and the right shoulder of the last mar are discernible.*

ticular coatings studied in detail here (*Figures* 11-13) made by the first method described. For example, presence of high shoulders in the cross-section in *Figure* 8 indicates that plastic deformation was a significant part of the marring mechanism. Other authors[21] reached similar conclusions based on scanning electron microscope images of similar mars. On the other hand, the absence of shoulders in *Figure* 9 indicates failure by fracture; the missing material is presumably accounted for by broken pieces removed by the cleaning procedure. *Figure* 10 suggests a mixture of failure mechanisms. The mar has shoulders, but the fact that the cross-section area of the shoulders appears less than the area of the ditch suggests that some fracture also occurred. *Figure* 12 shows the response of *coating PU* to the procedure described; here again, failure appears to have involved a mixture of plastic deformation and fracture. In contrast, the near absence of shoulders in *Figures* 11 and 13 indicate that the primary mechanism of marring of *coatings PE* and *AC* was fracture. The absence of shoulders might be explained by assuming that shoulders were formed initially but disappeared by viscoelastic creep during the hour between marring and characterization; however, this explanation seems unlikely because of the triangular shapes of the mars and because no appreciable change in the dimensions of these mars were noted when they were imaged again one to two weeks later. (While the dimensions of mars of the three coatings studied here do not change between one hour and several weeks, mars of certain other coatings do partially heal in this time frame.[21] Such coatings are currently under investigation in our laboratories).

The second marring procedure confirms these qualitative conclusions about marring mechanisms. *Figure* 14 illustrates the response of *coating PU* to the second marring procedure. In the cross-section profile, only one shoulder appears at one side of the tested area while the ditch and a second shoulder appear at the other side. The area in between appears almost unchanged. Remarkably, under these conditions, one shoulder made by each successive pass of the tip seems to have filled in the ditch made by each previous pass, smoothing the marred area. Small-scale viscoelastic creep may have also contributed to smoothing the surface of the marred area. The fact that the marred area is level with the unmarred surface indicates that virtually no fracture occurred under these conditions. The lines at the top and bottom of the test area in *Figure* 14 apparently consist of material pushed up by the tip when it reversed direction. In contrast, *Figure* 15 shows SPM images of the effect of its affect on *coating AC*. The rastering probe dug a square hole in the surface, showing that the primarly failure mechanism of this coating is fracture. As before, loose material from the hole was removed by the washing procedure.

### Quantitative Characterization of Responses to Marring Stress

Measurement of the cross-section areas, $A_{dit}$ and $A_{shs}$ for each mar was described previously (see *Figure* 16). The cross-section area $A_{ind}$ is not obtained from direct measurement of the mars. Rather, it is calculated from the dimensions of the tip of the high-modulus probe and the depth of its penetration into the coating surface during the micro indentation test using the same normal force used in making a particular mar. $A_{ind}$ must represent the cross-section of the depression swept by the probe as it scrapes through the material during the marring procedure.

Numbers representing the fraction of each of the three types of response resulting from a specific marring stress were calculated from these quantities by equations (2-4).

$$\%\ \text{Elastic response} = \frac{(A_{ind} - A_{dit})100}{A_{ind}} \quad (2)$$

$$\%\ \text{Plastic deformation} = \frac{(A_{shs})100}{A_{ind}} \quad (3)$$

$$\%\ \text{Fracture} = \frac{(A_{dit} - A_{shs})100}{A_{ind}} \quad (4)$$

In these equations area of mars made by a dynamic marring process are compared to an area ($A_{ind}$) of an indentation made in a static experiment. The dynamics of the two experiments may be different, and the areas may not be exactly comparable. Nonetheless, this method

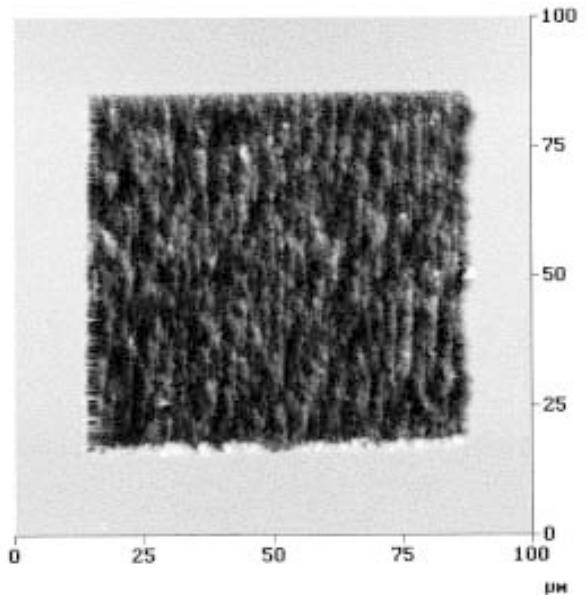


*Figure 15—A fracture dominant area of 70 μ x 70 μ after area marring.*

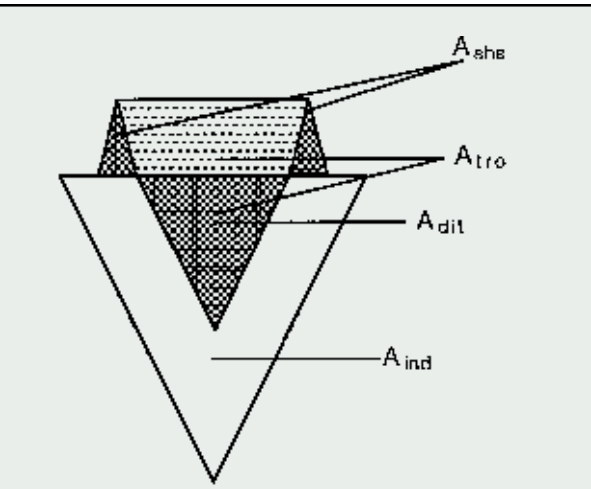


*Figure 16—Schematic illustration of how to measure different responses to marring in a quantitative way, and how to measure micro mar resistance.*

$A_{ind}$: Area of the cross-section of the indentation
$A_{dit}$: Area of the cross-section of the ditch
$A_{shs}$: Area of the two cross-section of the shoulders
$A_{tro}$: Area of the cross-section of the trough

Elastic Response: $(A_{ind} - A_{dit}) / A_{ind} * \%$
Plastic Deformation: $A_{shs} / A_{ind} * \%$
Fracture: $(A_{dit} - A_{shs}) / A_{ind} * \%$
Micro Mar Resistance: $F_N / A_{tro}$

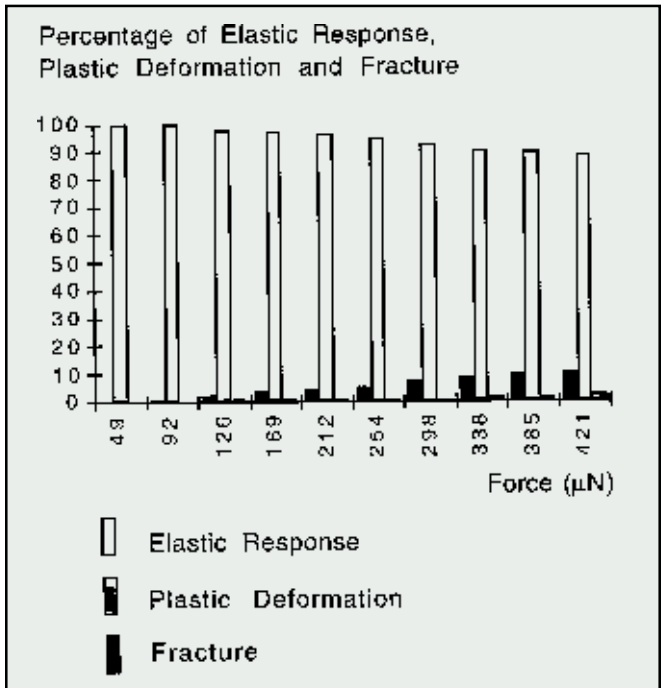


*Figure 17—Plot of elastic response, plastic deformation, and fracture versus the normal force for coating PE.*

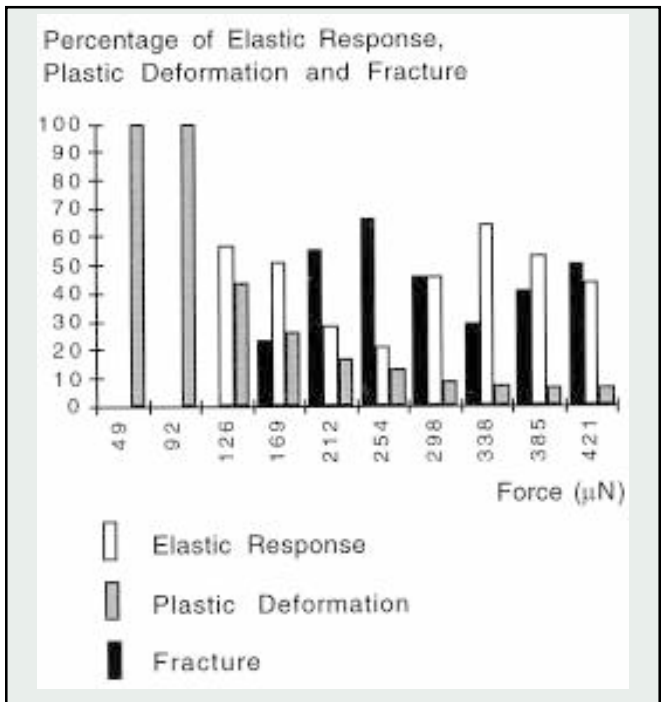


*Figure 18—Plot of elastic response, plastic deformation, and fracture versus the normal force for coating PU.*

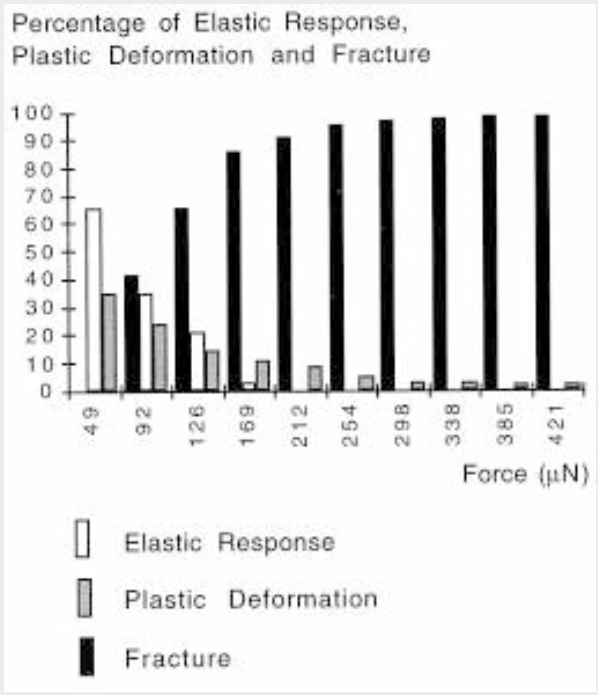


*Figure 19—Plot of elastic response, plastic deformation and fracture versus the normal force for coating AC.*

**Table 2—Micro Indentation Hardness in the Units N/(mm)² of Coatings PE, PU, and AC under 10 mN Normal Force at Indentation Depth of 1μ, 3μ, and 5μ Measured by H100 Micro-Hardness Tester**

| Indent Depth (μ) | Coating PE (N/mm*mm) | Coating PU (N/mm*mm) | Coating AC (N/mm*mm) |
|---|---|---|---|
| 1 | 11.3 | 208 | 200 |
| 3 | 9.1 | 153 | 125 |
| 5 | 10 | 140 | 111 |

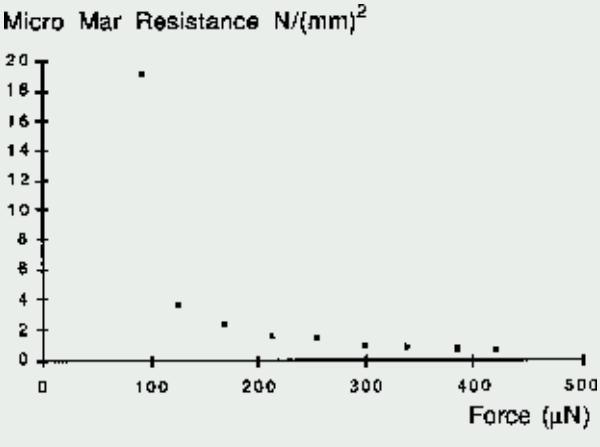


*Figure 20—Plot of micro mar resistance versus the normal force for coating PE.*

provides a quantitative index with which responses of different coatings can be compared. Its usefulness will be established only after a substantial number of coatings have been studied.

Results of calculations using equations 2-4 for the three coatings studied are given in *Table* 3 and are plotted in *Figures* 17-19. *Coating PE* has the most straightforward response, the elastic fraction being 100% of the response at an applied force of 49 μN and decreasing monotonically to 88% at the highest force tested. The excellent mar resistance of this material (demonstrated in the following) is attributable to its highly elastic response to marring forces. The balance of its response is mainly fracture, which rises from 0% to 10% as the marring force increases. Plastic deformation accounts for only 2% of the response of *coating PE* even at the highest force level examined.

The response of *coating PU* and *AC* are more complex. The response of *coating AC* (*Figure* 19) is about 2/3 elastic and 1/3 plastic at the lowest marring force, but it is dominated by fracture at forces of 254 μN and higher.

In contrast, the hard surface of *coating PU* (*Figure* 18) responds 100% by plastic deformation at the two lowest marring forces, but the plastic response is almost completely supplanted by a roughly equal mixture of elastic response and fracture as marring force increases. This observation may be related to the differences in composition of polyurethane coatings between the surface and the bulk detected by infrared spectroscopy.[34]

### Results of the Empirical Mar Resistance Test

In the Crockmeter test, *coating PE* had the best empirical scratch resistance, retaining 99% of its gloss. *Coating AC* retained 91% and *coating PU* retained 70%. Among contemporary auto finishes 70% would be marginally acceptable and 95% would be excellent. These results fall in the same rank order as the depth of the scratches observed in the SFM mar resistance test, especially if the height of the shoulders is added to the depth.

### Micro Mar Resistance

Because only two (plastic deformation and fracture) of the three responses to marring stress result in marring, we sought to define a single quantity that would reflect the combined magnitude of these two responses, that is, the dimensions of a mar under a certain normal force. This quantity is defined in equation (5).

$$\text{Micro mar resistance (MMR)} = \frac{F_N}{A_{tro}} \qquad (5)$$

Calculation of MMR uses $A_{tro}$ (the cross-section area of the trough, see *Figure* 16), defined as the cross-section area of the mar including the shoulders. It is $A_{dit}$ plus the area, if any, between the shoulders. $A_{tro}$ is defined in this way because it is theorized that it will correlate better than $A_{dit}$ with visual impressions of marring and with the optical measurements often used to assess marring. MMR is defined so that the highest numbers represent the best mar resistance under a given set of conditions.

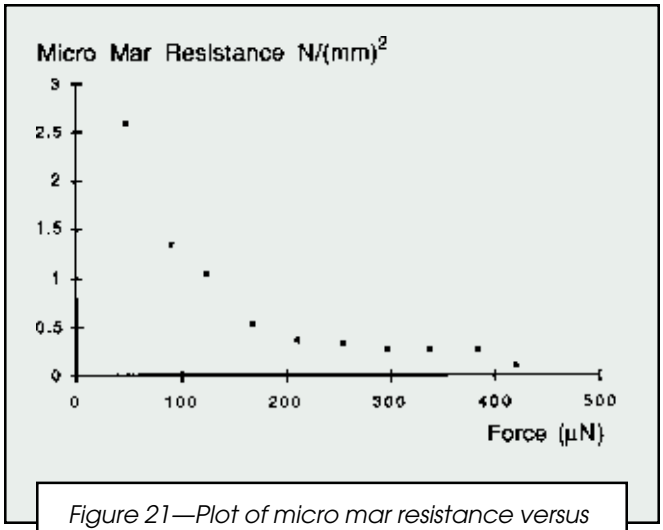


*Figure 21—Plot of micro mar resistance versus the normal force for coating PU.*

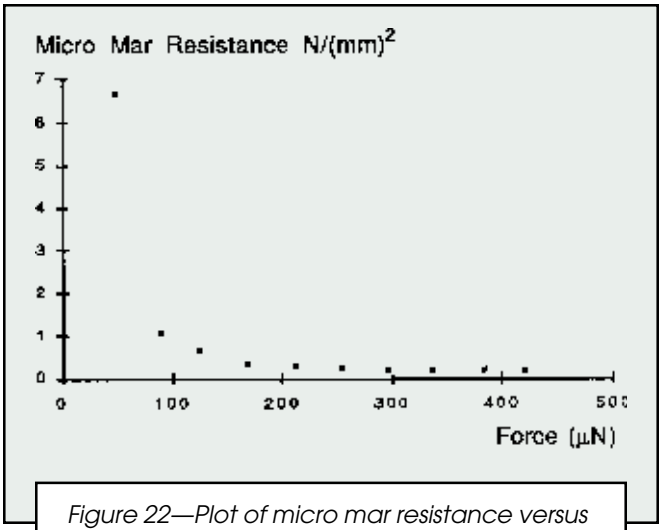


*Figure 22—Plot of micro mar resistance versus the normal force for coating AC.*

MMRs for the three coatings under the 10 normal forces tested are given in *Table* 4 and are plotted in *Figures* 20-22. Obviously, MMR for each coating depends strongly on the force applied for the measurement and presumably on all test condition variables such as temperature and rate of marring.

## DISCUSSION

An ideal mar resistant coating would resist marring under a wide variety of marring stresses in a wide temperature range. Such ideal coatings have been hard to find, and they will probably continue to be elusive. It is widely recognized that different materials vary widely in their ability to resist marring in different empirical tests and in service. Two important reasons are recognized: (1) In service there is enormous variation in the force with which marring stresses are applied; and (2) The response of a single coating may vary widely as the temperature and/or the rate of the application of stress are changed. The present study indicates that a third factor is also of major importance: (3) Many coatings have a gradient of responses in the few hundred nanometers closest to its surface.

Use of the SPM described here provides a new method for studying characteristics of polymeric materials including response gradients. This method is quite sensitive to differences in micro hardness of polymeric materials in the thin (100-500 nm) layer near the surface of the material. This could prove critically important if the behavior of *coatings PU* and *AC* prove to be representative of other coatings. These coatings apparently have thin crusts of material that are as much as 30 times harder than their bulk.

It is probably unrealistic to expect quantitative agreement of the microhardness results obtained by the new SPM method and conventional dynamic loading methods. The diamond tip of the high-modulus SPM probe is much smaller than the indenters used in dynamic loading methods, and the range of forces applied in dynamic loading methods and the depth of penetration are roughly an order of magnitude greater than with the SPM method. The more sensitive SPM method is capable of revealing differences in microhardness gradient in the 50-500 nm layer near the surface of materials that may not be detectable with the conventional dynamic loading method. For the materials studied here, microhardness near the surface is clearly a very complex phenomenon.

**Table 3—Percentages of Elastic Response, Plastic Deformation and Fracture of Coatings PE, PU, and AC Under 10 Different Normal Forces**

| Force (μN) | Coating PE | | | Coating PU | | | Coating AC | | |
|---|---|---|---|---|---|---|---|---|---|
| | % Elastic | % Plastic | % Fracture | % Elastic | % Plastic | % Fracture | % Elastic | % Plastic | % Fracture |
| 49 ..... | 100 | 0 | 0 | 0 | 100 | 0 | 65.1 | 34.9 | 0 |
| 92 ..... | 99.6 | 0.17 | 0.26 | 0 | 100 | 0 | 34.5 | 24.2 | 41.3 |
| 126 ..... | 97.7 | 0.26 | 2.08 | 56.7 | 43.3 | 0 | 20.8 | 14.1 | 65.1 |
| 169 ..... | 96.5 | 0.23 | 3.24 | 51 | 26.1 | 22.9 | 3.1 | 10.7 | 86.2 |
| 212 ..... | 95.7 | 0.45 | 3.87 | 28.4 | 16.6 | 55 | 0 | 8.76 | 91.2 |
| 254 ..... | 94.3 | 0.64 | 5.05 | 21.3 | 12.8 | 65.9 | 0 | 4.78 | 95.2 |
| 298 ..... | 92.2 | 0.82 | 6.97 | 45.5 | 8.7 | 45.8 | 0 | 2.95 | 97.1 |
| 338 ..... | 90.2 | 0.97 | 8.83 | 63.9 | 6.9 | 29.2 | 0 | 2.44 | 97.6 |
| 385 ..... | 89.4 | 1.25 | 9.35 | 53.1 | 6.4 | 40.5 | 0 | 21.3 | 97.9 |
| 421 ..... | 88.1 | 1.86 | 10 | 43.4 | 6.2 | 50.4 | 0 | 1.75 | 98.3 |

**Table 4—Micro Mar Resistance (MMR) of Coatings PE, PU, and AC under 10 Different Normal Forces**

| | Micro Mar Resistance | | |
|---|---|---|---|
| Force (μN) | Coating PE (x1000 N/mm*mm) | Coating PU (x1000 N/mm*mm) | Coating AC (x1000 N/mm*mm) |
| 49 | ∞ | 2.58 | 6.65 |
| 92 | 19.1 | 1.34 | 1.09 |
| 126 | 3.59 | 1.04 | 0.642 |
| 169 | 2.35 | 0.539 | 0.286 |
| 212 | 1.48 | 0.367 | 0.251 |
| 254 | 1.39 | 0.333 | 0.22 |
| 298 | 0.952 | 0.269 | 0.201 |
| 338 | 0.833 | 0.256 | 0.195 |
| 385 | 0.619 | 0.255 | 0.193 |
| 421 | 0.468 | 0.108 | 0.17 |

The complexities of measuring mar resistance can be no less than the complexities of measuring microhardness, and they are probably greater. The characteristics of the outer 100 to 300 nm of the surface must be critical because mars of this depth can be visible. Results presented here show that the response of the outer 100 nm of a material to marring stresses may be quite different from the response of the bulk material.

The behavior of *coating PU* (*Figure* 18) illustrates the point. This material has a thin, hard surface crust which undergoes a totally plastic response to weak marring stresses. More forceful stresses apparently penetrate the crust and reach an elastic region that can partly recover from the stress, but when it fails, it fails predominately by fracture. It seems possible that shallow mars in *coating PU* could heal on long standing,[21] especially if it is heated, by viscoleastic creep. However, it seems less likely that deeper scars could heal because they result predominately from fracture.

*Coating AC* has better empirical mar resistance than *coating PU*. This observation may be explained by its different responses to different levels of marring stress. The elasticity of its surface crust should protect it from visible marring under small stresses (see *Figure* 18). Under more severe marring stresses, *coating AC* fails mainly by fracture, while *coating PU* fails partly by plastic deformation. As a result, when the ditches of the mars of the two materials have comparable dimensions, the shoulders resulting from plastic deformation of *coating PU* may increase the optical impression of marring.

The excellent empirical mar resistance of *coating PE* can be attributed with some assurance to its highly elastic response down to a depths of at least 500 nm. Even severe marring forces dig deeply into its surface, but the material recovers most of its original dimensions, probably almost instantly after the probe has passed and certainly within one hour.

It remains to be established whether the newly proposed quantity micro mar resistance (MMR) will be useful for comparing mar resistance of coatings with optical tests and for gaining insight into how different marring forces affect different coatings. There is good reason to question whether any single quantity can represent the mar resistance of materials under a range of conditions. It is encouraging that *coating PE*, which performs best in the empirical Crockmeter test, also has the highest MMR of the coatings studied at all 10 force levels. However, MMRs for *coating AC* and *PU* correlate with Crockmeter results only at the lowest and highest normal forces. At intermediate normal forces *coating PU* has higher MMRs than *coating AC* although it performs less well in the Crockmeter test.

## CONCLUSIONS

The SPM modified with a high-modulus probe provides a promising new approach to the measurement of microhardness and of mar resistance of cross-linked materials. It provides a way to quantitatively measure three physical responses to marring stress, and to discriminate and measure two, quite different, mechanisms of marring. Differentiation of the mechanisms is expected to have practical significance. In any program to improve mar resistance of a coating, it should be useful to know whether marring results primarily from plastic deformation or from fracture in planning experimental strategy.

Our new methods are quite sensitive to differences in physical response in the thin layer near the surface. This sensitivity should help reveal nuances of the surface layer which may be especially important for study of mar resistance of coatings and other polymeric materials. Usefulness of these new methods will depend on the adequacy of the three response, two mechanism model to describe marring. Adequacy of this model and usefulness of the method can not be fully established until many more materials have been studied.

The apparent stratification observed in *coatings PU* and *AC* raises serious doubts about the feasibility of correlating bulk film mechanical properties with mar resistance for coatings that may have quite different mechanical properties near the surface. For example, it seems unlikely that the bulk elastic properties of *coating PU* will relate to the ability of the thin plastic layer on its surface (*Figure* 18) to resist marring. Furthermore, its bulk properties may have little relation to other surface properties, such as stain resistance.

In view of the great complexity of the physical response of polymeric materials to marring stresses, it seems impossible that a single quantity can express "the mar resistance" of a material. The best that can be hoped for is that a single quantity might be useful for comparing mar resistance of different materials under a carefully specified set of conditions. In this vein we offer micro mar resistance, a quantity that might prove useful. It combines the two mechanisms of marring into a single quantity. Its advantage over most empirical tests is that it can be measured under controlled conditions.

## ACKNOWLEDGMENTS

Support of this research by the National Science Foundation Industry/University Cooperative Research Center in Coatings at Eastern Michigan University, Michi-

gan Molecular Institute, and North Dakota State University, by the Research Excellence Fund of Eastern Michigan University, and by Ford Motor Company is gratefully acknowledged.

## References


(1) Shen, W., Ji, C., Jones, F.N., Everson, M.P., and Ryntz, R.A., "Measuring Scratch Resistance and Microhardness of Crosslinked Coatings with a Scanning Force Microscope," *Polymer Mater. Sci. Eng*., 74, 346-347 (1996).

(2) Shen, W., Ji, C., Jones, F.N., Everson, M.P., and Ryntz, R.A., "Measurement by Scanning Force Microscopy of the Scratch and Mar Resistance of Surface Coatings," *Surface Coat. Intl. 1996*, 6, 253-236 (1996).

(3) Courter, J.L., "Mar Resistance of Automotive Clearcoats: I. Relationship to Coating Mechanical Properties," JOURNAL OF COATINGS TECHNOLOGY, *69*, No. 866, 56 (1997).

(4) Anon., "Standard Test Method for Mar Resistance of Organic Coatings," *Amer. Soc. Test. Mater*., Method D 5178-91.

(5) Briscoe, B.J., "Tribology of Polymers: State of an Art," in *Physicochemical Aspects of Polymer Surfaces*, Mittal, K.L. (Ed.), Plenum, Vol. 1, pp. 387-412, New York (1983).

(6) Briscoe, B.J., Evans, P.D., and Lancaster, J.K., in *Wear of Materials*; Ludema, K.C. (Ed.), The American Society of Mechanical Engineers, Vol. 2, pp. 607-618, New York (1987).

(7) Briscoe, B.J., Evans, P.D., and Lancaster, J.K., "Single Point Deformation and Abrasion of y-Irrdiated Poly(tetrafluoroethylene), *J. Phys. D*., 20, 346-353 (1987).

(8) Briscoe, B.J., Pelillo, E., and Sinha, S.K., "Characterization of the Surface Deformation, Yield, and Fracture of Polymers During Scratching," *Proc. 10th Intl. Conf. On Deformation, Yield, and Fracture of Polymers*, Cambridge, UK, 474-477, United Kingdom (1997).

(9) Balta Calleja, F.J., "Microhardness Studies of Polymers and Transitions," *Trends Polymer Sci.,* 2, (12), 419-425 (1994).

(10) Balta Calleja, F.J., "Microhardness Relating to Crystalline Polymers," *Adv. Polymer Sci*., 66, 117-148 (1985).

(11) Balta Calleja, F.J., Martinez-Salazar, J., and Rueda, D.R., "Hardness," in *Encyclopedia of Polymer Science and Engineering*, Kroschwitz, J.I. (Ed.), John Wiley and Sons, Vol. 7, pp 614-626, New York (1987).

(12) Lamy, B., "Effect of Brittleness Index and Sliding Speed on the Morphology of Surface Scratching in Abrasive or Erosive Processes," *Tribol. Int*., 17 (1), 35-38 (1984).

(13) Lawn, B.R. and Howes, V.R., "Elastic Recovery at Hardness Indentations," *J. Mater. Sci*., 16, 2745-2752 (1981).

(14) A. Ya. Gol'dman, *Prediction of the Deformation Properties of Polymeric and Composite Materials*, translated by M. Shelef and R.A. Dickie, ACS Professional Reference Books, American Chemical Society, Washington, D.C., 1996.

(15) Mai, Y-W. and Cottrell, B., "On the Essential Work of Ductile Fracture in Polymers," *Int. J. Fracture*, 32, 105-125 (1986).

(16) Darlix, B., Monasse, B., and Montmitonnet, P., "Hardness Measurement as a Means of Determining Simultaneously the Elastic Modulus and Yield Stress of Polymers as a Function of Temperature," *Polymer Test*, 6 (2), 107-120 (1986).

(17) Nordstrom, J.D., "Automotive Clearcoats Incorporating Silane Functionality and Auxiliary Crosslinkers," *Proc. 22nd Intl. Waterborne, High-Solids, and Powder Coat. Symp.,* 22, 492-501, New Orleans (1995).

(18) Jacobs, P.B. and Engbert, T., "Scratch and Mar Resistance of Polyurethane Automotive Clearcoats," *Proc. 5th Ann. ESD Adv. Coat. Conf. Expo.,* The Engineering Society, 29-39, Ann Arbor, MI (1995).

(19) Morse, M.P., in *Paint and Coatings Testing Manual*, Koleske, J.V. (Ed.) American Society for Testing and Materials, pp. 525-533, Philadelphia, PA (1995).

(20) Gregorovich, B.V. and McGonigal, P.J., "Mechanical Properties of Coatings Needed for Good Scratch and Mar," *Proc. Adv. Coat. Tech. Conf. ASM/ESD*, pp 121-125, Materials Park, OH (1992).

(21) Betz, P. and Bartelt, "Scratch Resistant Clear Coats: Development of New Testing Methods for Improved Coatings," *Prog. Org. Coat*., 22, 27-37 (1993).

(22) Sano, S., Yamada, K., and Ishihara, M., "Relationship Between Viscoelastic Property and Scratch Resistance of Topcoat Clear Films," *Toso Kagaku*., 29 (12), 475-480 (1994).

(23) McGinniss, V.D., "Developing Abrasion-Resistant Coatings," *Paint & Coat. Ind*., 34-39 (1994).

(24) Tonge, J.S., Blizzard, J.D., Schmidt, S.M., and Washer, T.R., "Microhardness in UV Cured Abrasion Resistance Coatings," *Proc. 22nd Intl. Waterborne, High-Solids and Powder Coat. Symp*., 22, 432-439, New Orleans, LA (1995).

(25) Garey, H.E., "Optically Clear Light Stable Polyurethanes for Scratch Resistant Films on Glass and Plastic, *J. Elastomers Plast*., 17 (2), 119-131 (1985).

(26) Shibato, K., Beseche, S., and Sato, S., *Proc. PRA Fourth Asia-Pacific Conference*: "Advances in Coatings, Inks, and Adhesives," Hong Kong, Paint Reserach Association, International Centre for Coatings Technology, Paper 4, 1994.

(27) Chen, M.J., Osterholtz, F.D., Phol, E.R., and Ramdatt, P.E., "Silanes in High Solids and Waterborne Coatings," *Proc. 23rd Intl. Waterborne, High-Solids and Powder Coat. Symp*., 23, 222-233, New Orleans, LA (1996).

(28) Kahl, L., Halpaap, R., and Wamprecht, "2C-PU Automotive OEM Clear Coats with Improved Etch and Scratch Resistance," *C. Surf. Coat. Int/JOCCA*, 76 (10), 394-399 (1993).

(29) Evans, R.M., in *Treatise on Coatings*, Myers, R.R. and Long, J.S. (Eds.), Marcel Dekker, Vol. 2, Part I, pp 13-190, New York (1969).

(30) Heilen, W., *Pigm. Resin Technol*., 22 (4), 10-15 (1993).

(31) Kody, R.S. and Martin, D.C., "Quantitative Characterization of Surface Deformation in Polymer Composites Using Digital Image Analysis," *Polymer Eng. Sci*., 36 (2), 298-304 (1996).

(32) Weiler, W.W., "A New Microhardness Test Method," *J. Test. Eval*., 18 (4), 229 (1990).

(33) McGhie, A.J., Tang, S.L., and Li, S.F.Y., "Expanding the Uses of AFM," *Chemtech,* 20-26 August, 1995.

(34) Kaminski, A.M. and Urban, M.W., "Quantitative Analysis of Urethane Films Near Surfaces and Interfaces," *Polymer Mater. Sci. Eng*., 75, 110 (1996)